

Quantitative Interpretation: Use of Seismic Inversion Data to Directly Estimate Hydrocarbon Reserves and Resources

James Shadlow*

KUFPEC Australia
7/100 Railway Road
Subiaco WA 6008

James.shadlow@kufpec.com.au

Adam Craig

KUFPEC Australia
7/100 Railway Road
Subiaco WA 6008

adam.craig@kufpec.com

David Christiansen Robert Mitchell

KUFPEC Australia
7/100 Railway Road
Subiaco WA 6008

David.christiansen@kufpec.com

KUFPEC Australia
7/100 Railway Road
Subiaco WA 6008

Robert.mitchell@kufpec.com

**presenting author asterisked*

SUMMARY

A quantitative interpretation workflow utilising AVO inversion based lithology prediction data was developed to directly assess reserves and resources for an LNG development project in the Carnarvon Basin. The study area is covered by modern MAZ PSDM 3D seismic data using broadband acquisition and processing techniques, calibrated by numerous well intersections of the Triassic Mungaroo Formation reservoirs.

Interpretation of the fluvio-deltaic reservoir bodies can be somewhat interpretive using 'traditional' workflows. By interpreting chronostratigraphic events tied to well-based biostratigraphy and then using the lithology prediction volumes, the interpretation of reservoir bodies becomes more objective.

Seismic inversion data are typically used to qualitatively guide resource assessments, through amplitude mapping or use in static and dynamic modelling. In this case study, the inversion based prediction volumes are used to extract P90, P50 and P10 sand geobodies which are directly input into probabilistic reserve and resource assessments. The workflow is applied to discovered, developed, undeveloped and prospective reservoirs.

Geobody extraction required the PSDM depth data to be accurately calibrated to wells. A calibrated velocity model was built by perturbing the imaging velocities in a 3D model to tie the chronostratigraphic events associated with all the reservoir intervals. Fluid contacts derived from wells were used to provide a depth cut-off to the geobody extractions.

The resulting reserve and resource assessments from this workflow show an excellent match with previous assessments including static and dynamic modelling methods. The geobodies also identified previously unrecognised channel sands not easily interpreted on full and angle stack data.

Key words: Seismic Inversion, Lithology prediction, Probabilistic Reserves,

INTRODUCTION

The Julimar-Brunello field complex in Production License WA-49-L, Carnarvon Basin comprises 29 separate accumulations of oil and gas in the Upper Triassic fluvio-deltaic reservoirs of the Mungaroo Formation in three fault-bound traps. The fields are situated at the southern-most tip of the Rankin Trend, south of the Pluto field and northeast of the Gorgon field (Figure 1). Brunello is the northern most complex of pools, located on a horst. The Grange pool is a faulted anticline in a graben on the Main Horst complex directly southwest of Brunello. The Julimar pool complex is situated on a horst to the south of the Grange Graben. Each accumulation exhibits a component of stratigraphic seal, where the hydrocarbons are reservoired in fluvial channel sands.

Twenty-eight chronostratigraphic events have been identified on well correlations to define the main reservoir units, and these events can be interpreted over the study area on the 2014 Harmony-Joy broadband Multi-Azimuth (MAZ) pre-stack depth migrated (PSDM) 3D seismic survey (HJ14). The 3D survey covers 562 km². There are 46 well penetrations of the Triassic within the 3D area, of which 38 have been used for correlation purposes (Figure 1). The reservoirs are stratigraphically located between the TR30.1 TS and the TR20 SB (Marshall & Lang, 2013). Only the shallowest eight reservoirs in the northern Brunello field (Four reservoirs within WA-49-L) share a common contact; all other reservoirs have discrete hydrocarbon and aquifer pressure gradients and fluid contacts. The Brunello accumulations commenced development in 2014 and are currently being produced through the Wheatstone platform and LNG facilities.

Interpretation of fluvial channels within a single reservoir unit with one known fluid contact can be reasonably straight forward. However, interpretation of channel geometries for the volumetric assessment for 29 pools spread over 3 structures in 28 reservoir intervals, where different channels in one chronostratigraphic interval show different fluid contacts in wells becomes very time consuming and interpretationally subjective. The subjectivity is due to channel edges not always being readily identifiable, thin channel associated reservoir not always being recognised and intra-channel heterogeneities affecting the amplitude response. In addition, the predominant class 3 AVO effect exhibited by the Mungaroo reservoirs (Al-Duaij et al. 2013) complicates the interpretation of channels near the fluid contacts.

Seismic inversion data is commonly used in conjunction with reservoir static and dynamic modelling to help constrain reserve assessments, and has been effectively used both on the Julimar Brunello complex (Al-Duaij et al. 2013) and on the Gorgon Field to the southwest (Van Der Weiden, Nayak, & Swinburn, 2012). In addition, there are several case studies in which inversion data has been used to de-risk exploration (Di Luca, et al., 2014), calculate net pay (Alvarez et al. 2014), or use stochastic inversion to assess sand connectivity in a simulation model (Moyen & Doyen, 2009). Previous work has shown that AVO inversion and lithology – prediction methods can assist in distinguishing gas from brine sands in this study area (Lamont, Thompson, & Bevilacqua, 2008). Inversion based prediction volumes were generated as part of the HJ14 processing project, where ties were made to the 29 exploration and appraisal penetrations of the Julimar-Brunello horst. The remaining 9 penetrations from oil and gas development wells could therefore be used as blind tests. Given the complexities of using conventional methods to assess the reserves and resources, the merits of using the lithology and fluid prediction cubes to define the gross-rock volumes (GRV) range in a probabilistic reserves assessment were investigated without resorting to a geo-cellular modelling approach.

PSDM depth images result in the best imaging solution, but do not always give the best depth model of the subsurface (Etris, Crabtree, & Dewar, 2002). Even with the widespread usage of anisotropic tomography to update the PSDM velocity models, the final image may not tie the wells (O'Neill & Thompson, 2016). In this study area, it was found that the TTI PSDM velocity model had misties at the reservoir level of up to 30m, in part due to shallow carbonates and in part due to a 20m velocity model sample rate being similar to the thicknesses of the reservoirs. Therefore, prior to hydrocarbon contact depth consistent geobody extraction, the imaging velocities needed to be adjusted to minimise the depth errors for all the chronostratigraphic tops in all the wells.

Traces from the lithology and fluid prediction volumes were extracted at each well, and the tie to wells was assessed. Statistical analysis of the 134 sands intersected in the wells indicated that the P90 and P10 estimates of sand prediction matched with the 90th and 10th percentile of sand presence in wells. This confirmed that the input rock physics modelling to the inversion and prediction process was reasonable. Using these cut-offs and the fluid contact information, geobodies were extracted for the Julimar, Grange and Brunello areas for each stratigraphic interval as input to the estimate of probabilistic reserves and contingent resources for the permit. This approach removed some of the subjectivity of the interpretation, and ensured thin pay, encountered in some wells but previously not included in reserves assessments, was captured in the reserves estimation.

METHOD AND RESULTS

The ultimate goal of the study was to estimate the reserves and resources for the Julimar Brunello complex using the lithology / fluid prediction volumes in the depth domain to define the probabilistic GRV range. However, for this to be meaningful, the velocity model is required to result in depth images that tie the wells. Seeing as this was not the case in this study area, regional events picked in sufficient detail were required to be interpreted to enable a well-tied velocity model to be generated. Well control is essential to define what seismic events were required to be interpreted. The approach applied is summarised in Figure 2

Well Correlations

Historically, the Brunello horst, Grange graben and Julimar horst have been interpreted in isolation, with limited understanding of the regional connectivity of sands and pressures between them. However, to be able to use the prediction volumes for GRV estimation, a velocity model that tied to all the wells covered by the 3D area was required to ensure the best seismic to well depth match was achieved so that the fluid contact information could be meaningfully applied. In addition, the regional reservoir distribution and impact of Intra-Mungaroo Formation marine flooding events was not well understood. Therefore, the first step was to correlate all the wells, using the biostratigraphy data and regional seismic mapping as a guide (Figure 3 (Shadlow, Craig, & Christiansen, 2016).

This correlation built up a series of well based chronostratigraphic tops that corresponded to the top of reservoir sequences in most wells. It also resulted in the chronostratigraphic tops being interpreted in the floodplain or overbank facies. It was noted that the overall N:G estimated from the gamma ray logs were slightly higher (e.g. subtle GR decrease) in the overbank facies compared to the surrounding shales (Figure 3). The overbank facies chronostratigraphic tops were made based on biostratigraphic data, consistency in the isopach thicknesses from well to well and match with seismic ties.

Seismic – Well Ties and Seismic Interpretation

Detailed seismic synthetics were estimated for each well, tying the HJ14 PSDM full stack data (3 – 35 degrees) in the time domain. Checkshot surveys were recorded in most wells and, where absent, an average was generated from surrounding wells as a starting point. Synthetics were generated using a SEG-Normal (increase in impedance = peak graphically or positive number mathematically) zero-phase Ricker wavelet, matched to the dominant frequency in the Triassic at the well. Generally, the checkshot data showed a very good match to the seismic, although some small shifts were required to tie the Jurassic Oxfordian unconformity (JO). Stretch and squeeze shifts to explicitly tie all sands to the seismic were not done as these were generally small (<5ms). A zero phase Ricker wavelet was chosen as the well data is be zero phase, and the aim of synthetic generation is to estimate the time and phase mistie to seismic. Using a statistical wavelet at each well has the potential to provide an unstable estimate of the overall polarity of the seismic data. However, it should be noted that a multi-well statistical wavelet was estimated for the inversion process, where the result showed a good match to a Ricker wavelet (Figure 4).

The HJ14 PSDM full stack data was interpreted in time, where troughs (decrease in impedance) corresponding to each chronostratigraphic formation top were interpreted. This resulted in a set of 28 Triassic events being interpreted regionally across the Julimar – Brunello area for use in velocity modelling, attribute analysis and geobody extraction.

Velocity Modelling

The starting velocity model chosen was the TTI PSDM imaging velocities that had been geostatistically kriged by the processing company to provide an optimal tie to the wells. Although the synthetic analysis showed that the time data matched the checkshot data reasonably well, it was found that misties were as large as $\pm 40\text{m}$ (Figure 5). This error is due to the geostatistical tie process only being controlled by the JO surface; no intra-Triassic events were used as input. In addition, issues previously discussed relating to shallow carbonates and the large velocity sample intervals are thought to contribute to the errors. Therefore, a new velocity model was required to minimise the depth errors at the wells, so that fluid contact information could be used as a depth constraint for geobody calculation. If the inversion prediction models mistie the wells in depth, then these contact data could not be used.

Given the proximity of interpreted events (every seismic trough), and the magnitude of the errors, a layer-independent depth conversion approach could not be applied, as the tied grids could potentially cut over grids above and below. Even though there are many wells in the area, the most penetrations of any single stratigraphic layer was twelve, resulting in sub-optimal sampling of most layers. Therefore, by applying the corrections in 3 dimensions, correction trends from shallower layers are applied to deeper layers. Furthermore, depth tied grids were not sufficient, as a 3D velocity model was required to convert the lithology and fluid prediction 3D seismic volumes to depth. Therefore, a 3D velocity model was generated, using the geostatistically kriged PSDM velocities, formation tops and chronostratigraphic picks as input. The velocity modelling was conducted using Petrel, and corrections were applied in 3D using a least-squares error minimisation approach.

Analysis showed that 206 of the 317 formation tops (Sand and floodplain) had a resultant error of less than $\pm 5\text{m}$, and that 278 tops had errors between $\pm 15\text{m}$. Furthermore, the tops where sands were identifiable using petrophysical analysis showed that 97 of 134 events had errors of less than $\pm 5\text{m}$. These residual errors are thought to be due to small errors in seismic picking (sample rate 4ms, 5m), gridding errors by introduced by slight smoothing of the grids and pick uncertainty in the “floodplain” areas where the seismic events were not as strong or continuous. Therefore, the velocity model was deemed to be suitable for providing a good tie to wells for geobody extraction.

Lithology / Fluid Prediction volume analysis and geobody extraction

Once the regional chronostratigraphic events had been interpreted and a velocity model that resulted in good well ties in depth has been generated, it is possible to commence extracting geobodies. However, the cut-off applied to

extract the geobodies becomes critical to ensure that the range of GRVs estimated by the geobodies correspond with the P90, P50 and P10 confidence in sand presence.

The prediction volumes were generated by stochastic modelling of the rock physics modelling to generate depth-dependant estimates of sand probability, based on extraction of elastic properties from well log data (Figure 6). The modelling was conducted in AI - Vp/Vs crossplot space, and the depth dependant probability density functions (PDFs) were applied to the absolute AI and Vp/Vs inversion volumes. Note that the PDFs encompass 2 standard deviations from the mean, or 95% of all data. Therefore, some sands should not be predicted by inversion. Also note that the oil and gas ellipses almost exactly overlie, due to the high GOR of the oils encountered in this area. For the purposes of prediction, it was decided to combine these two ellipses together to estimate the hydrocarbon sand.

Before any analysis could be performed, it was observed that a hydrocarbon prediction was always encased in a “brine” sand prediction (Figure 3, Figure 7). The hydrocarbon sand prediction and brine sand predictions were combined using

Equation 1. This combination ensured that if a geobody cut-off was based on a brine sand cut-off, there would not be a hole in the middle of the geobody corresponding to a hydrocarbon sand prediction. This equation also implies that any sand encountered above the contact must be hydrocarbon filled, and that a “brine” prediction must relate to either thinner or poorer quality sand.

Equation 1: Total sand prediction estimate from brine sand and hydrocarbon sand volumes.

After generation of a total sand prediction volume, all traces within 50m of each borehole were extracted and averaged for statistical comparison of the prediction volumes with presence of actual sand. We reviewed the average, peak (maximum) and “integral” (area under curve) of each trace and found that the peak value gave the best correlation to sand thickness. The average estimate smeared out resolution as it convolved both thickness and maximum values. The integral estimate retained information from both, but is difficult to extract from the seismic data. In addition, the peak value can be combined with the geobody thickness to estimate the integral. Review of the histogram of the peak prediction value results in several observations (Figure 8):

1. The distribution is tri-modal, corresponding roughly to floodplain areas, water bearing sands and hydrocarbon bearing sands.
2. 90% of sands with Sw<50% show a prediction value of greater than 0.9. The values less than 0.9 correspond to oil reservoirs (2 predictions at 0.6), poor quality gas sand (1 prediction at 0.7) and thin sands beneath the major eastern fault (0.1-0.3 points). Therefore, it is possible to be 90% confident of encountering a gas sand above the contact when the prediction is greater than 0.9. In addition, no well in the study area that intersected a prediction greater than 0.9 failed to find reservoir quality sand.
3. 10% of all intersected sands have a total sand prediction less than 0.1; this has been used to define the cut-off for the P10 GRV geobody extraction
4. Several wells are highly deviated. These were removed from the analysis for simplicity, but generally show the same trends as the vertical well data.
5. Assessment of P90 and P10 from statistical analysis is in agreement with prediction volume values, indicating that the rock physics modelling and low frequency modelling of the inversion data is fair and reasonable.

Using the cut-offs of 0.9 for the P90 and 0.1 for the P10, P90 and P10 confidence geobodies were extracted for all chronostratigraphic zones above the free-water levels in the Julimar, Brunello and Grange areas (Figure 9). A P50 estimate was also generated using a cut-off of 0.5, and this P50 showed very good agreement with a Monte Carlo Log-normal P50 estimate generated using the P90 and P10 values. The geobodies showed good agreement with the interpretation of channels from seismic, but also identified several areas of thin pay not mapped previously. Review of well intersections in these zones has identified petrophysical pay that had previously been ignored (Figure 10).

One potential issue identified related to the sand thickness estimates at the wells, where traditionally tuning prohibits estimates of thickness from geobodies. In the approach presented here, the amplitude effect from tuning has theoretically been removed, where the tuning thickness occurs between 20-25m. By using different amplitude cut-offs, the different geobodies essentially lie on a series of discrete amplitude – thickness curves. It was found that the P90 geobody consistently under-predicted reservoir thickness compared to wells, while the P10 consistently over-predicted (Figure 11). The P50 showed a reasonable match, where the scatter is contained within a single standard deviation (+33%). It is worth noting that the traditional approach of channel interpretation on seismic reflection data is also impacted by seismic tuning effects.

Petrophysics, Fluid Properties and Dynamic Factors

Petrophysical analysis that was undertaken as part of the inversion study was also used to define average properties and ranges for reservoir properties. It was found that sands encountered in a “floodplain”: setting still exhibit similar net-to-gross and porosity properties as sands in the main channels, although obviously the gross thickness was much less. Many of the penetrations occurred near the free-water level, so a crossplot of gas saturation and porosity all reservoirs above the transition zone was made to estimate the water saturation range. This showed a good cluster of points, with a trend of decreasing Sg with decreasing porosity evident.

Gas samples acquired from the exploration, appraisal and development wells facilitated assessment of the fluid properties required for the reserve and resource assessment (including the gas expansion factor and condensate yield).

The results of historical reservoir models underpin the recovery factor range applied in the Monte Carlo assessment. Lower recovery factors are expected in scenarios where a strong aquifer is present whereas higher recoveries can be achieved in depletion drive scenarios. The recovery factor range was modified for the layers where the connectivity of the entire accumulation to the development well/s (or proposed development location) was uncertain.

Reserves & Resource Comments

Monte Carlo probabilistic Reserves and resources were calculated numerically using the Rose and Associates software. No dependencies between layers were assumed. The approach presented here made no attempt to explicitly estimate a P50 or best technical estimate case. Rather, the P50 outcome was defined by the P90 and P10 inputs. The approach was also applied consistently across all reservoirs, except for the Balnaves Oil reservoir, where a P90 cut-off of 0.7 was applied in agreement with the statistical analysis (Figure 8). No interpretational bias relating to channel edge definition has been introduced. The resulting reserves and contingent resources estimate was slightly more optimistic when compared with legacy static and dynamic modelling results.

Pitfalls

Low saturation gas has been interpreted in 2 reservoirs, but the lithology / fluid prediction volumes show that hydrocarbon bearing reservoir is expected. Therefore, this method does not resolve the well-established low-saturation gas problem with the seismic method. Furthermore, some wells have intersected gas prediction anomalies down-dip from established contacts and encountered water. The false gas prediction in these cases is attributed to the presence of very clean, very porous sands. Water bearing reservoir of these type of sands have been intersected several times in the study area. In 2 cases, wells have intersected “brine sand” predictions above the established contact, and encountered water. In these cases, the prediction shows that the wells intersected a stratigraphically separate channel from where the gas discovery was made. As such, care must be taken in inferring a common contact across different discrete channels in a single chronostratigraphic interval.

CONCLUSIONS

Conducting a probabilistic reserves assessment using inversion volumes appears straight forward at first glance. However, as with any geological and geophysical evaluation, data preparation and assessment of data quality is critical. In this case study, we could make an estimate of the probabilistic reserves and contingent resources for a very complex group of fields without going through the rigours of a full static and dynamic model, which resulted in a significant time saving. However, a significant amount of time was spent on the well correlations and generating the velocity model to ensure that the depth volumes tied the wells adequately. The method presented here removed the requirement for the interpreter to objectively interpret sand channels across many reservoir units and structural compartments, resulting in an increase in the reserves estimate due to the addition of net sand. This approach also allowed for uncertainty estimation in both sand thickness and lateral extent away from well control to be conducted in a systematic manner.

ACKNOWLEDGMENTS

We wish to thank KUFPEC for permission to publish this data and the WA-49-L Joint Venture. We'd also like to thank DownUnder Geosolutions for undertaking the inversion processing and petrophysical analysis that was used for this work.

REFERENCES

- Al-Duaij, E., Al-Maraghi, M., Zaid, T., & Klopf, T. (2013). Application of seismic attributes in estimating gas resources in complex fluvial channel reservoirs. SPE Kuwait Oil and Gas Show and Conference. Kuwait: SPE.
- Alvarez, P., Bolivar, F., Marin, W., Di Lucas, M., & Salinas, T. (2014). Seismic Quantitative interpretation of a gas bearing reservoir - From rock physics to volumetric. EAGE Conference and Exhibition. 76. Amsterdam: EAGE.
- Di Luca, M., Salinas, T., Arminio, J. F., Alvarez, G., Alvarez, P., Bolivar, F., & Marin, W. (2014, July). Seismic inversion and AVO analysis applied to predictive-modeling gas-condensate sands for exploration and early production in the Lower Magdalena Basin, Colombia. *The Leading Edge*, 33(7), 746-756. doi:10.1190/tle33070746.1
- DownUnder Geosolutions. (2014). Harmony Joy QI Report. Perth: DownUnder Geosolutions.
- Etris, E. L., Crabtree, N. J., & Dewar, J. (2002, November). True depth conversion: more than a pretty picture. *CSEG Recorder*, 26(9).
- Geoscience Australia. (2015). Regional Geology. Retrieved June 28th, 2017, from Offshore Petroleum Exploration Acreage Release, Australia 2015: <http://archive-petroleumacreage.industry.slicedtech.com.au/2015/geology/northern-carnarvon-basin/geology>
- Lamont, M. G., Thompson, T. A., & Bevilacqua, C. (2008). Drilling success as a result of probabilistic lithology and fluid prediction a case study in the Carnarvon Basin, WA. APPEA, 1-12.
- Marshall, N. G., & Lang, S. C. (2013). A new sequence stratigraphic framework for the North West Shelf, Australia. West Australian Basins Symposium. Perth: PESA.
- Moyen, R., & Doyen, P. M. (2009). Reservoir Connectivity uncertainty from stochastic seismic inversion. SEG Technical Program Expanded ABSTRACTS (pp. 2378-2382). Houston: SEG. doi:10.1190/1.3255337
- O'Neill, A. J., & Thompson, T. A. (2016, October). Improved depth conversion with FWI - a case study. *First Break*, 34(10), 85-89.
- Shallow, J. M., Craig, A. J., & Christiansen, D. C. (2016, June). Is there a benefit to throwing the kitchen sink at geotechnical studies in an exploration phase. *The APPEA Journal*, 56(1), 203-218. doi:10.1071/AJ15015
- Van Der Weiden, R., Nayak, P., & Swinburn, P. (2012, September). Seismic technology supporting reserves determinations: Gorgon field, Australia. *The Leading Edge*, 31(9), 1050-1058. doi:10.1190/tle31091050.1

Figures and Tables

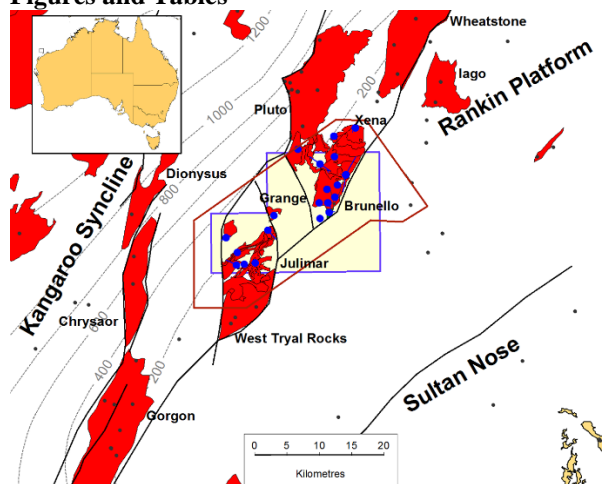


Figure 1: Location map showing WA-49-L production license in yellow, HJ14 3D seismic coverage in maroon, regional gas fields in red and structural features in black. Wells shown in grey, and wells used for the study shown in blue. Bathymetric contours are shown in grey. Modified from Geoscience Australia (2015).

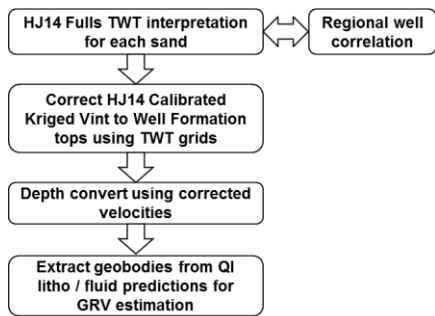


Figure 2: Interpretation workflow applied to estimate GRV using geobodies extracted from the prediction volumes.

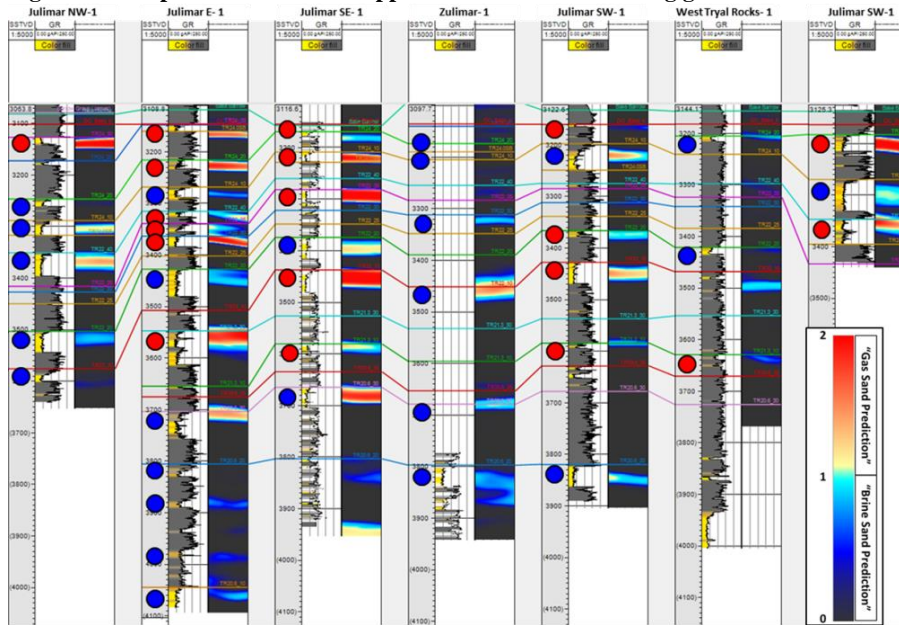


Figure 3: Well correlation in the Julimar area showing gamma-ray and depth tie to total sand prediction volumes using well tied velocity model. Gas sands are annotated with red circles and brine sands with blue circles. Note that formation tops correspond to subtly lower gamma-ray response where sands not clearly interpreted.

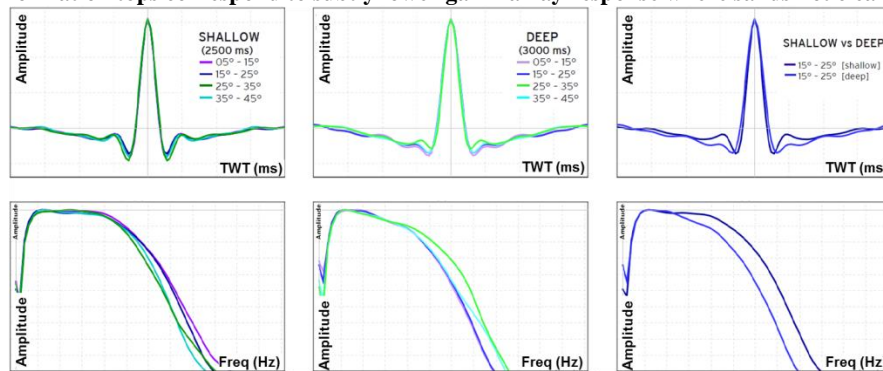


Figure 4: Multi-well statistical wavelets extracted for use in inversion. Note wavelets show data is zero-phase and can be well approximated by a Ricker Wavelet. Modified from DownUnder Geosolutions (2014).

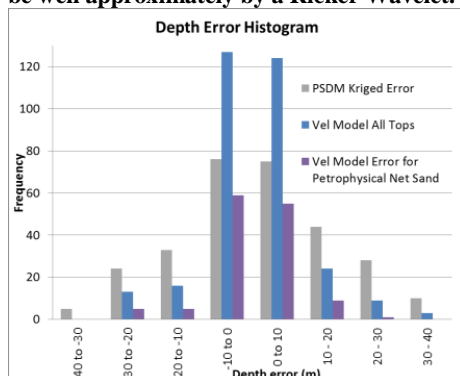


Figure 5: Depth error histogram for all formation tops using the PSDM Kriged velocities (grey), all formation tops using corrected velocity model (Blue) and all formation tops where net sand was identified during petrophysical evaluation (purple).

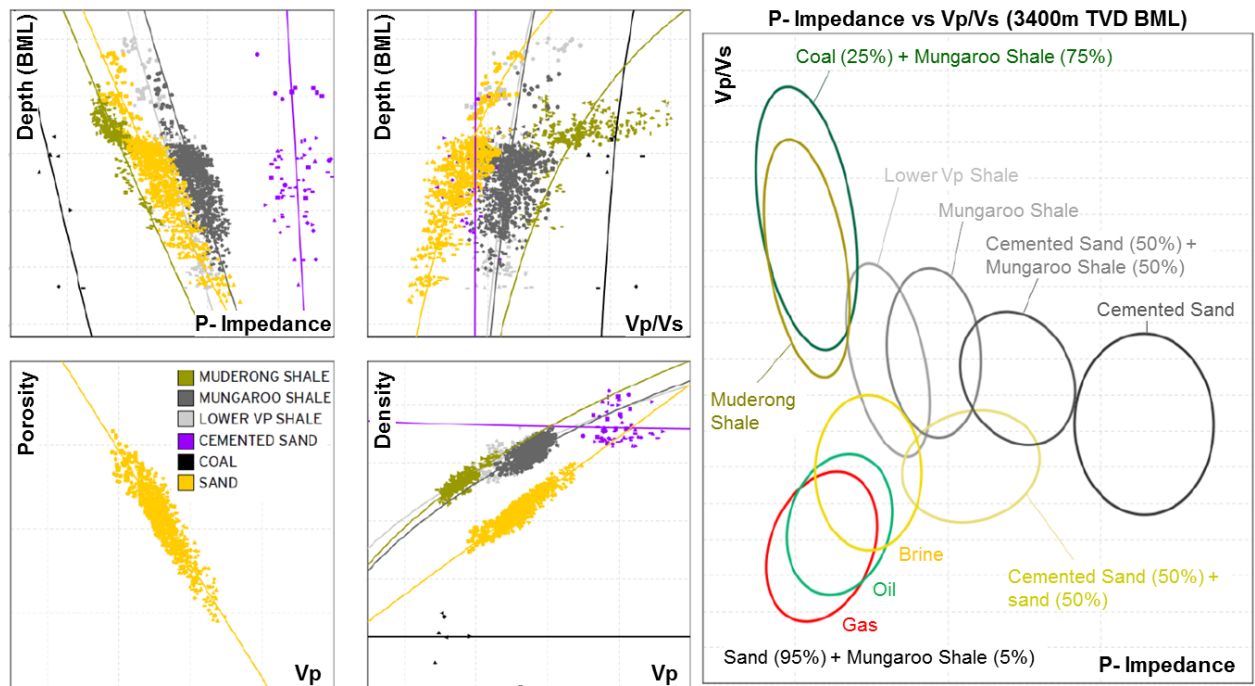


Figure 6: Example plot of PDF generation at 3400m below mud line (BML) from rock physics depth trends, used to generate lithology and fluid prediction volumes. Modified from DownUnder Geosolutions (2014).

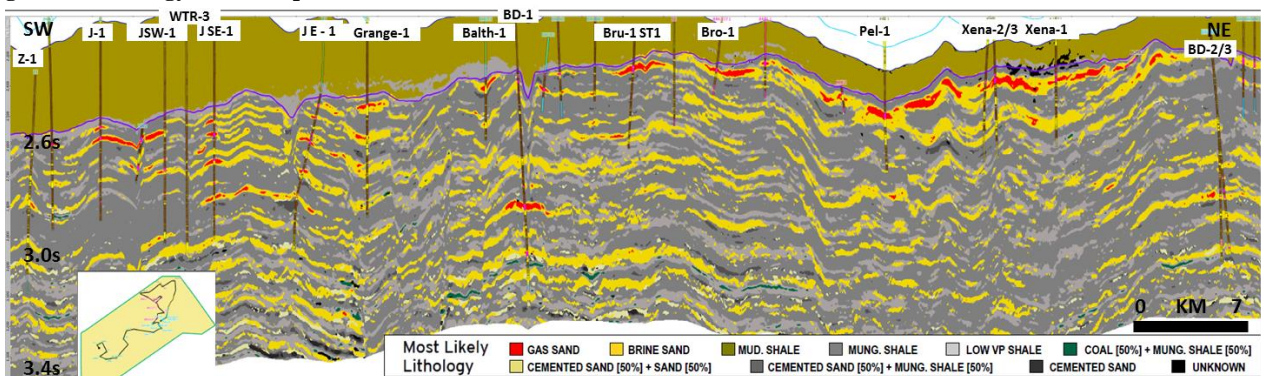


Figure 7: Arbitrary line through key wells extracted from HJ14 3D, showing most likely lithology prediction. Note that the hydrocarbon prediction is always encased in a brine prediction. Modified from DownUnder Geosolutions (2014).

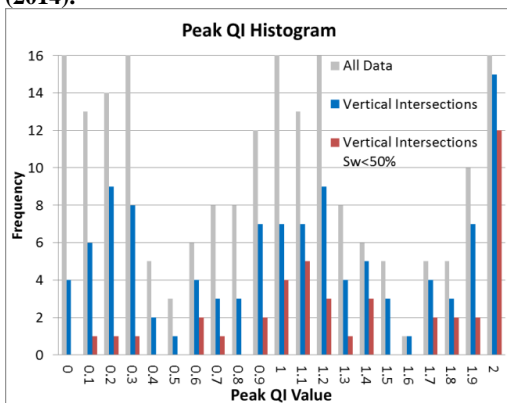


Figure 8: Histogram showing peak QI prediction for all wells and all chronostratigraphic levels. Scale is such that the 0.1 bar captures peak predictions in range from 0-0.1. Note that 90% of sands with water saturation less than 50% plot above 0.9. Also note that 90% of all sands plot above 0.1.

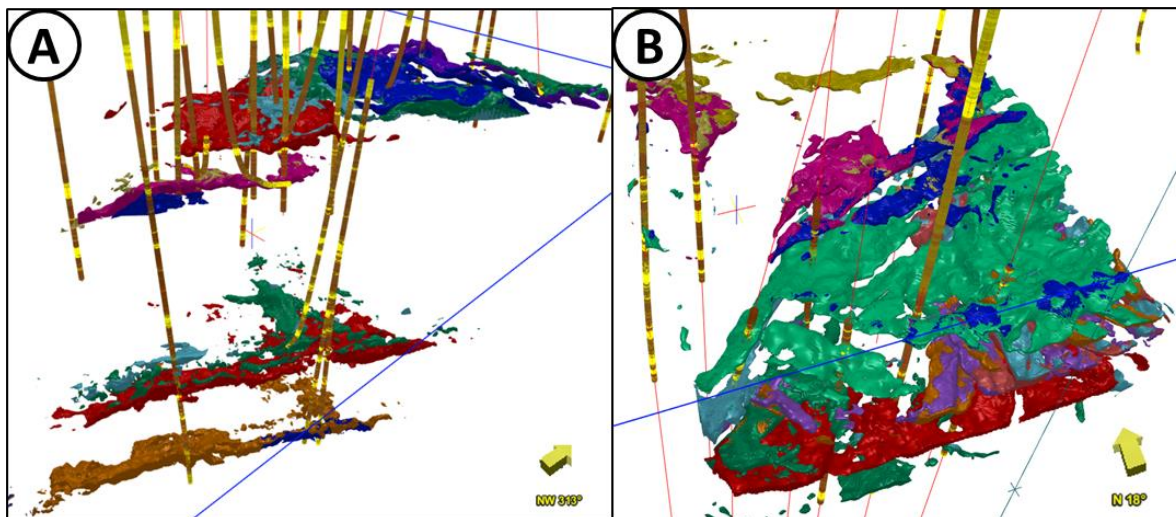


Figure 9: P50 geobody extractions for (A.) Brunello field and (B.) Julimar field. Each different coloured geobody is a different reservoir.

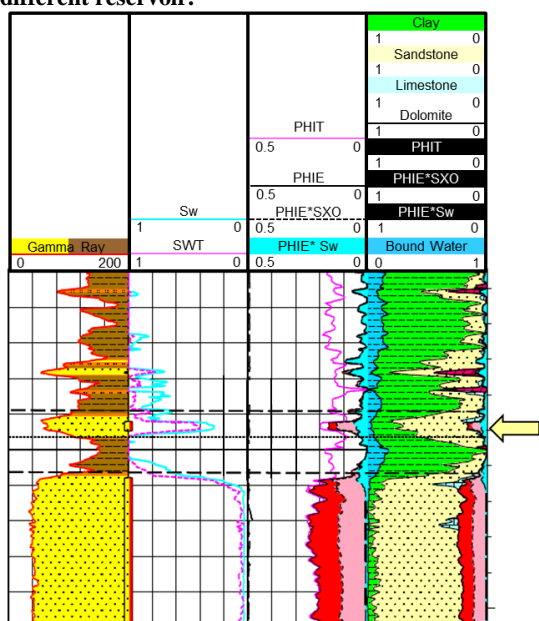


Figure 10: Petrophysical analysis from a well showing thin sand with pay above thicker gas sand. This thin interval is mappable on seismic and is connected to thicker channels elsewhere.

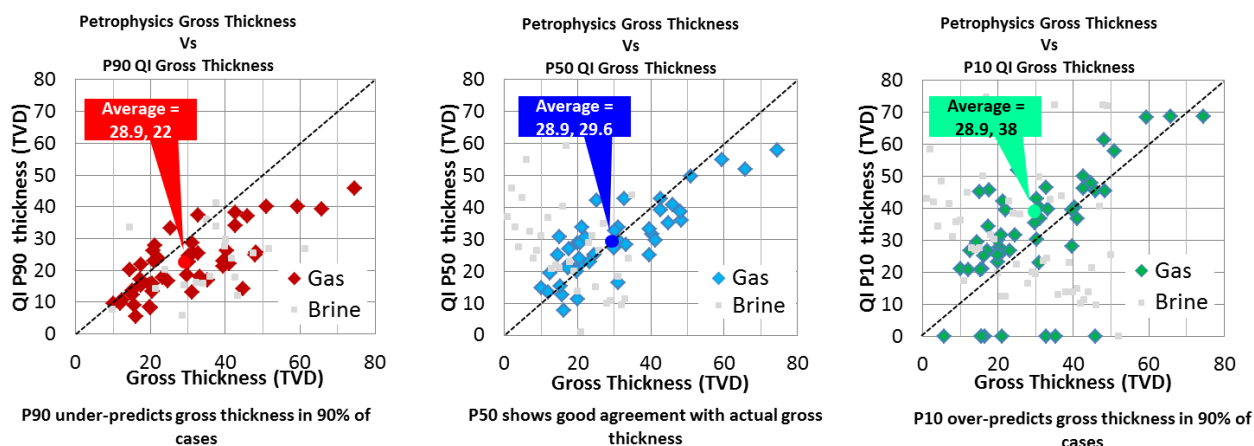


Figure 11: Comparison of well gross thickness with the QI extracted thickness at each well. The P90 under-predicts sand thickness in 90% of cases, and the P10 over-predicts sand thickness in 90% of cases.